Vibration and Thermal Energy Harvesting System for Automobiles with Impedance Matching and Wake-up

Ji Hoon Hyun, Long Huang, and Dong Sam Ha Multifunctional Integrated Circuits and Systems (MICS) Group Bradley Department of Electrical and Computer Engineering Virginia Tech, Blacksburg, Virginia, 24061, USA {jhyun, longh93, ha}@vt.edu

Abstract—This paper presents a system for vibration and thermal energy harvesting from automobiles, and it intends to power wireless sensor nodes. Two main features of the proposed circuit are impedance matching to extract maximum power and wake-up to incorporate sleep mode. Two separate buck-boost converters in discontinuous conduction mode are used for impedance matching. A wake-up circuit senses the vibration energy generated by a piezoelectric cantilever (PZT). When a car is turned off, the wake-up circuit deactivates the two converters, and the entire circuit goes into sleep mode to save power. The proposed circuit charges a capacitor to power a wireless sensor node, and is able to cold start. The proposed circuit is prototyped with discrete components. Experimental results show that the proposed system harvests peak power of 3.4 mW and these results also demonstrate that a wireless sensor node can be powered by the proposed system.

Keywords—Energy harvesting (EH) from automobiles. wake-up circuit, impedance matching, vibration energy harvesting, thermal energy harvesting.

I. INTRODUCTION

Energy harvesting from ambient energy has attracted immense research interests for wireless sensor nodes [1]-[9]. Energy harvesting intends to eliminate the need to replace or recharge batteries, so wireless sensor nodes can operate perpetually [10]-[14].

Bloomberg New Energy Finance expects that the sale of electric vehicles would reach 41 million by 2040, which accounts for 35% of light duty vehicle sales [15]. The report also predicts that electric vehicles would cost the same as gasoline-based ones by 2022. Electric vehicles and driverless cars require a large number of sensors, and hard-wired sensors are expensive to install and maintain and take up large spaces [16]. Wireless sensor nodes powered by ambient energy is a promising solution to the problem.

Vibration and thermal gradient are widely available for automobiles. Zhu et al. investigated vibrations of a moving vehicle under various conditions [17]. The vibration frequency ranges between 12 Hz and 30 Hz, and the acceleration is as large as 1 g for a vehicle moving at the speed of 30 km/h. Tak and Setia explored harvesting energy from the waste heat of automobile engines, and showed feasibility to light up headlights through thermal energy harvesting under the temperature gradient of 70 °C [18].

Privately owned cars are parked about 95% of the time [19]. When cars are not in operation, it is desirable to turn off an energy harvesting circuit for power saving. It necessitates a wake-up circuit. Vibration energy harvesting circuits for piezoelectric cantilevers (PZT) often adopt a nonlinear method called Synchronized Switch Harvesting on Inductor (SSHI) [20]-[22] and Maximum Power Point Tracking (MPPT) [23]-[24]. However, SSHI and MPPT lead to high circuit complexity, and hence, may be suitable only for IC implementations [20]-[22], [25].

In this paper, we present a vibration and thermal energy harvesting system from automobiles. It adopts resistive impedance matching with buck-boost converters operating in discontinuous conduction mode (DCM). A wake-up circuit senses the energy level generated by a PZT and controls the operation mode of the proposed circuit. The circuit is able to cold start, meaning it can start even if the power storage capacitor is completely drained. This paper is organized as follows. Section II reviews relevant materials. Section III presents the proposed energy harvesting system and describes implementation of a wake-up circuit. Section IV presents experimental results of the proposed system. It also demonstrates the ability of the proposed system to power a wireless sensor node. Section V draws a conclusion.

II. PRELIMINARIES

A. Multi-Source Energy Harvesting

Multi-source energy harvesting increases the amount and reliability of the harvested power [26]-[28]. Design challenges of multi-source energy harvesting include incorporating wide ranges of input voltages from different sources and different characteristics of source impedances [27], [28].

Alhawari et al. investigated a wearable system to harvest vibration and thermal energy from a human body and to power a biomedical processor [26]. The system adopts a passive rectifier for a PZT and a boost converter for a thermoelectric generator (TEG). It is able to cold-start out of vibration energy, but does not adopt impedance matching. Multi-source energy harvesting systems for solar, vibration, and thermal energy are proposed in [27] and [28]. Bandyopadhyay and Chandrakasan adopted impedance matching for individual transducers. Energy is harvested from one source at a time, which enables sharing of the inductor to reduce the size [27]. In contrast, Ding et al. harvested energy from three different sources simultaneously

using three separate converters [28]. Neither of the designs considers wake-up and cold-start.

B. Negative Voltage Converter

A PZT requires rectification, and a full bridge rectifier. A rectifier made of passive diodes including Schottky diodes dissipates relatively large power for a small scale energy harvesting system. The negative voltage converter (NVC) shown in Fig. 1 performs rectification while reducing the power dissipation [29]-[33]. During the positive half cycle of the input voltage, PMOS transistor M_1 and NMOS transistor M_4 are turned on, and the current flows from node A through M_1 to the load and flows back to node B through M_4 . It is opposite for the negative half cycle. The diode D_1 prevents reverse flow of the current from the load if the load voltage (such as the load battery

voltage) is higher than the source voltage. The drain-to-source voltage drop of a turned-on transistor is small to result in low power dissipation of an NVC. Note that the direction of the body diodes of the transistors coincides with the direction of the current.

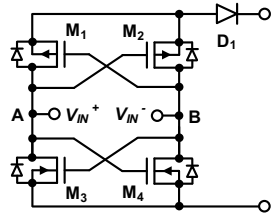


Fig. 1. NVC circuit.

C. Impedance Matching

An inverting buck-boost converter is shown in Fig. 2, where the polarity of the output voltage is opposite to the input voltage. The emulated input resistance of a buck-boost converter in DCM is given in (1)

$$R_{IN} = \frac{2L}{D^2 T_s} \tag{1}$$

where L is the inductance, D is the duty cycle, and T_S is the switching period of the converter. The input impedance of an ideal buck-boost converter in DCM is independent of the operating conditions, such as input and output voltages and load resistance. An inverting buck-boost converter is adopted for impedance matching for the proposed circuit and others such as [23] and [34].

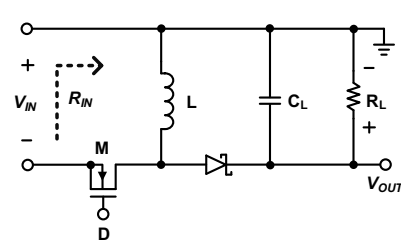


Fig. 2. Inverting buck-boost converter topology.

III. PROPOSED ENERGY HARVESTING SYSTEM

This section presents the proposed system for vibration and thermal energy harvesting from automobiles and explains wakeup and impedance matching circuit design.

A. Overview

A PZT and TEG are used for the proposed system, and the proposed system intends to power a wireless sensor node. A

block diagram of the proposed system is shown in Fig. 3. The major building blocks are an NVC rectifier, a wake-up circuit, two buck-boost converters with associated oscillators, and a buck converter to regulate the output voltage.

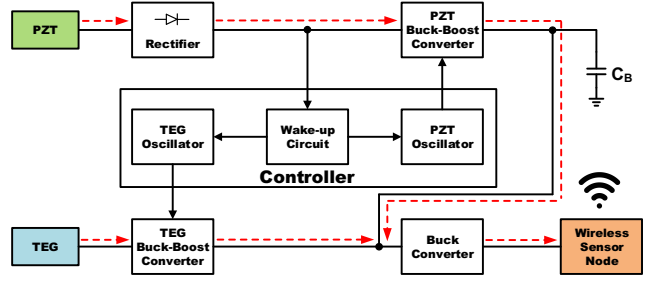
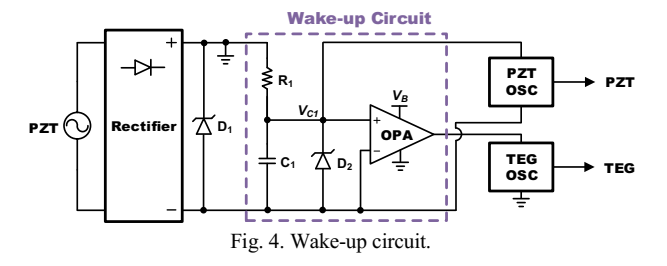


Fig. 3. Block diagram of the proposed system.

When a car is in operation, the PZT generates AC voltage, which is rectified by the NVC rectifier. Upon sensing the NVC output voltage, the wake-up circuit activates the PZT and TEG oscillators by providing power to the two oscillators. Each oscillator generates a sequence of pulses with a constant duty cycle and a fixed frequency, which activates the associated buck-boost converter. The input impedance of a buck-boost converter matches the source impedance based on the formula (1). The two converters share the same load and a capacitor C_B, and the energy harvested by a PZT and/or TEG charges the capacitor independent of the energy harvesting status of the other transducer. The buck converter regulates the output voltage to 1.8 V to power a wireless sensor node.

B. Wake-up Circuit

The wake-up circuit shown in Fig. 4 consists of an RC filter with R_1 and C_1 , a difference amplifier (OPA), and a Zener diode D_2 . The NVC rectifies AC voltage, and the RC low pass filter reduces the ripple. When the voltage V_{CI} across the capacitor C_1 reaches 0.9 V, the PZT oscillator (denoted as "PZT OSC" in the figure) powered by the capacitor C_1 becomes active, which in turn activates the PZT buck-boost converter. The vibration energy captured by the PZT starts to charge the capacitor C_B shown in Fig. 3. When the capacitor voltage V_B reaches to 1.6 V, the difference amplifier, powered by the capacitor voltage V_B , is active. The difference amplifier in turn activates the TEG oscillator and hence the TEG buck-boost converter. The thermal energy captured by the TEG also starts to charge the capacitor C_B . The Zener diodes D_1 and D_2 limit the maximum corresponding voltages for protection.



Let's consider the cold start capability of the proposed system. Suppose that the capacitor C_B is drained completely, and all the blocks are deactivated. As the PZT generates voltage out of vibrations, the NVC becomes active to charge the capacitor C_1 . When the capacitor voltage V_{CI} reaches to 0.9 V,

it activates the PZT oscillator. The oscillator in turn activates the PZT converter to harvest the vibration energy, which starts to charge the capacitor C_B . As the capacitor voltage reaches 1.6 V, it activates subsequently the difference amplifier OPA, the TEG oscillator, and the TEG converter.

Finally, it is feasible to share the oscillator for both PZT and TEG. However, sharing the oscillator does not reduce the overall circuit complexity due to the opposite polarity of the output voltage of an inverting buck-boost converter.

C. Impedance Matching

Two separate inverting buck-boost converters operating in DCM are used for impedance matching for the PZT and TEG. In order to obtain the target impedance of the PZT or TEG, a variable resistor is connected directly to the transducer, and the optimal resistor value R_{OPT} is obtained through the measurement of the power of the variable resistor. The duty cycle D of the switch in Fig. 2 is obtained from (1) and given below.

$$D_{OPT} = \sqrt{\frac{2Lf_s}{R_{OPT}}} \tag{2}$$

where f_s is the switching frequency. The switching frequency and the inductor L are determined considering several design issues, such as loss and size.

The overall circuit diagram of the proposed system is shown in Fig. 5. An oscillator generates the switching signal with the desired duty cycle for the associated buck-boost converter. Refer to [23] for details of the oscillator design. The two buck-boost converters charge the same capacitor C_B , and the output voltage V_{OUT} is regulated to 1.8 V with an off-the-shelf buck converter LTC3405A-1.8. As the diode D_1 blocks reverse flow of the current from C_B to the NVC, a diode at the output of the NVC is unnecessary, and hence, eliminated.

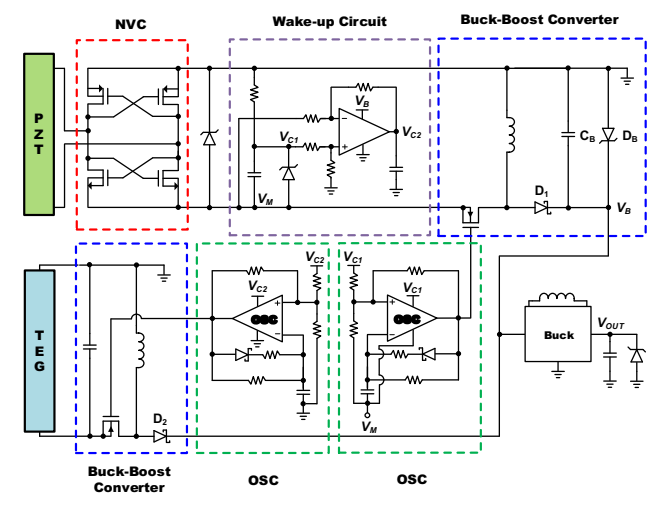


Fig. 5. Proposed energy harvesting system diagram.

IV. EXPERIMENTAL RESULTS

A. Prototype and Experiment Setup

The proposed energy harvesting circuit is prototyped with commercial off-the-shelf components and is shown in Fig. 6 (a). The experiment setup is shown in Fig. 6 (b), in which the

prototyped system powers a wireless sensor node from harvested energy. The PZT and TEG used for the experiments are Mide PPA-1001 and Thermal Electronics TEG2-126LDT, respectively. The PZT with a tip mass of 23 grams is vibrated with the RMS acceleration of 0.6 g at the resonant frequency of 15 Hz in the experiment. The temperature gradient of the TEG is set to 5 $^{\circ}$ C.

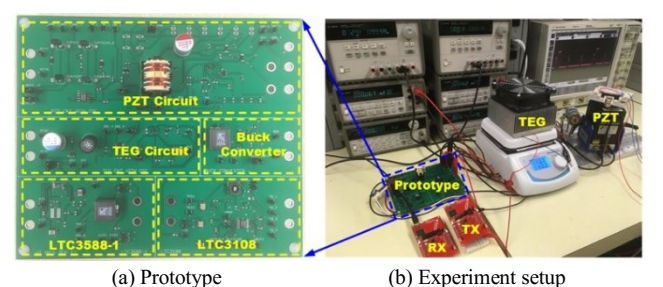


Fig. 6. Prototype and experiment setup.

B. Power and Efficiency of Vibration Energy Harvesting

A resistor is connected directly to the PZT alone without any other circuits, and the power delivered to the resistor is measured and shown in Fig. 7(a). The measurement result shows that the peak power of 4.52 mW is achieved for the resistance of 80 k Ω , and the maximum power is used as the reference power to calculate the efficiency of the proposed system for vibration energy harvesting. The power is sensitive to the resistor value, which indicates that impedance matching is necessary for vibration energy harvesting with a PZT.

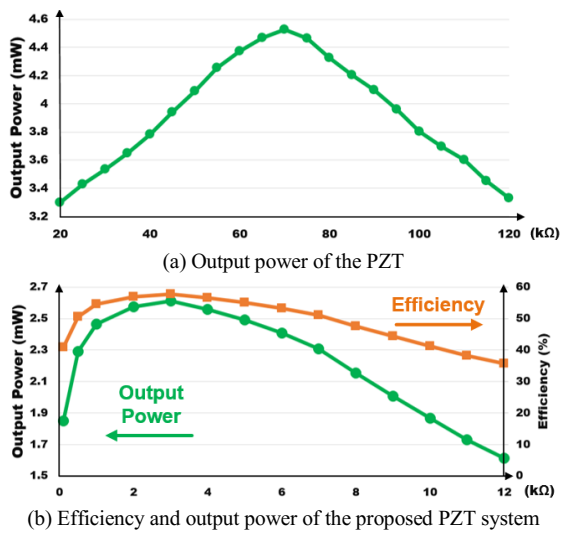


Fig. 7. Vibration energy harvesting system alone.

Next, the power and efficiency of the proposed system for vibration energy harvesting is measured. To emulate the optimal resistance of $80 \text{ k}\Omega$, the duty cycle of the PZT buckboost converter with a 22 mH inductor is set to 2.9% under the switching frequency of 1.52 kHz. The TEG buck-boost converter, the associated oscillator, and the buck converter at the output are deactivated. A variable load resistor is attached in parallel with the capacitor C_B . The power delivered to the load resistor is measured and shown in Fig. 7(b) along with its

efficiency. The efficiency is obtained as the reference power of 4.52 mW to the power delivered to the load resistor under the vibration energy harvesting system alone. The peak efficiency and output power of the PZT converter are 57.7% and 2.61 mW, respectively, under the load resistance of 3 k Ω .

C. Power and Efficiency of Thermal Energy Harvesting

We performed the same measurement for thermal energy harvesting. A resistor is connected directly to the TEG alone, and the power delivered to the resistor is shown in Fig. 8(a). The peak power of 5.22 mW is achieved for the resistance of 5.5 Ω . Similar to the PZT case, the output power is sensitive to the resistor value, and so it needs impedance matching. To emulate the optimal load resistance of 5.5 Ω , the duty cycle of the TEG buck-boost converter with a 390 μ H inductor is set to 45.2% under the switching frequency of 1.44 kHz. The efficiency and power delivered to the load resistor for the proposed thermal energy harvesting system alone is shown in Fig. 8(b). The peak efficiency and output power of the TEG converter are 55.6% and 2.9 mW, respectively, under the load resistance of 3 k Ω .

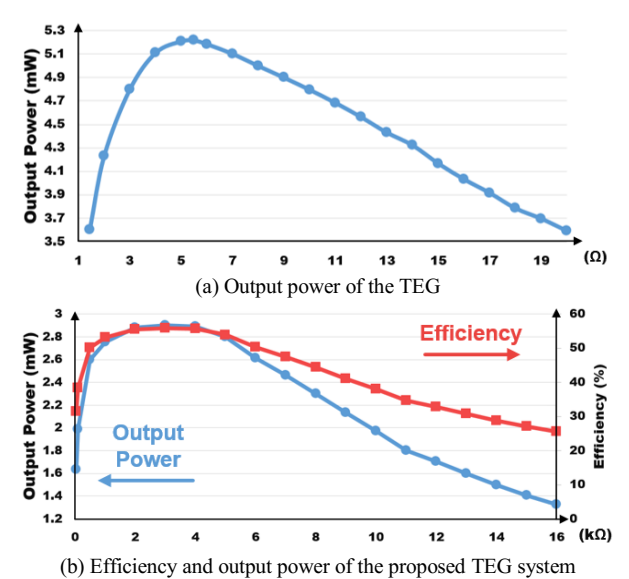


Fig. 8. Thermal energy harvesting system alone.

D. Power and Efficiency of the Proposed System

We prototyped a circuit with the same function using commercial off-the-shelf energy harvesting ICs, LTC3588-1 for vibration energy harvesting and LTC3108 for thermal energy harvesting. The two outputs of the ICs are connected together through Schottky diodes and their output voltage is regulated to 1.8 V using a buck converter IC, LTC3405A-1.8, which is, in fact, also used for the proposed circuit. Fig. 9 compares the measured power of the two systems. The proposed system harvests 3.4 mW in peak for the load resistance of 1 k Ω , while the prototype harvests 1.7 mW under the resistance of 2 k Ω . The efficiency of the proposed system is higher than the prototype by two times. The output voltage for the proposed system is maintained at 1.8 V for the load resistance greater than 1 k Ω , while it is 2 k Ω for the prototype.

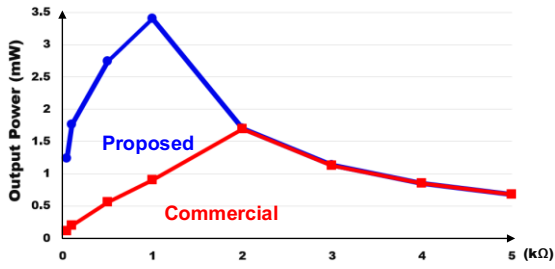


Fig. 9. Output power of the proposed and the prototype systems.

E. Wireless Sensor Node

A wireless sensor node is developed with a TI CC1310 microcontroller (MCU) LaunchPads with an embedded Zigbee radio. The wireless sensor node is powered by the proposed energy harvesting system. The sensor node samples the signals of eight channels with a sampling rate of 100 Hz, and its primary application is to monitor battery cell voltages. Fig. 10 shows the waveforms of the source voltage, the received and reconstructed voltage, and the MCU current of the transmitter. The signals of eight channels are sampled during Δt_1 (=1 ms) and transmitted during Δt_3 (=2 ms). The standby time Δt_2 (=9 ms) is the interval between two adjacent actions, and the MCU is in the standby mode for 16% of the operation period. The average current of the MCU is 1.9 mA to result in average power dissipation of 3.4 mW under the supply voltage of 1.8 V. The proposed system harvests sufficient energy to power the wireless sensor node.

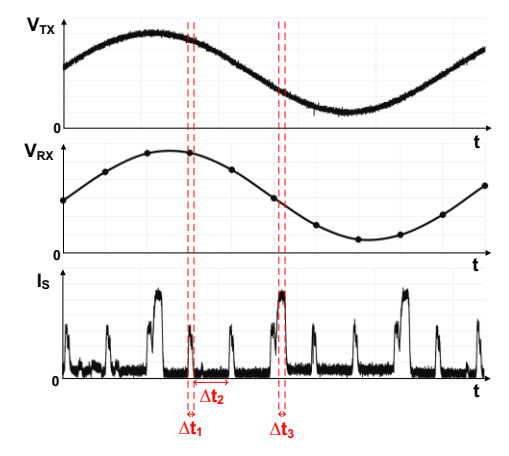


Fig. 10. Waveforms of the wireless sensor node.

V. CONCLUSION

An energy harvesting system for vibration and thermal energy harvesting from automobiles is presented in this paper. Two main features of the proposed system are impedance matching and wake-up. The efficiency of the proposed system is higher than a prototype with commercial energy harvesting ICs by two times. Experimental results show that the proposed system can power a wireless sensor node under automobile environments.

ACKNOWLEDGMENT

This work was supported in part by the Center for Integrated Smart Sensors funded by the Ministry of Science, ICT & Future Planning as Global Frontier Project" (CISS-2-3).

REFERENCES

- Q. Brogan, T. O'Connor and D. S. Ha, "Solar and thermal energy harvesting with a wearable jacket," 2014 IEEE International Symposium on Circuits and Systems (ISCAS), Melbourne VIC, pp. 1412-1415, 2014.
- [2] M. R. Elhebeary, M. A. A. Ibrahim, M. M. Aboudina and A. N. Mohieldin, "Dual-Source Self-Start High-Efficiency Microscale Smart Energy Harvesting System for IoT," in *IEEE Transactions on Industrial Electronics*, vol. 65, no. 1, pp. 342-351, Jan. 2018.
- [3] S. Fan, L. Zhao, R. Wei, L. Geng and P. X. L. Feng, "An ultra-low quiescent current power management ASIC with MPPT for vibrational energy harvesting," 2017 IEEE International Symposium on Circuits and Systems (ISCAS), Baltimore, MD, pp. 1-4, 2017.
- [4] T. Ruan, Z. J. Chew and M. Zhu, "Energy-Aware Approaches for Energy Harvesting Powered Wireless Sensor Nodes," in *IEEE Sensors Journal*, vol. 17, no. 7, pp. 2165-2173, April 2017.
- [5] Z. J. Chew and M. Zhu, "Combined power extraction with adaptive power management module for increased piezoelectric energy harvesting to power wireless sensor nodes," 2016 IEEE SENSORS, Orlando, FL, pp. 1-3, 2016.
- [6] W. Liu, Z. Wang, S. Qu and R. Luo, "Vibration energy harvesting and management for wireless sensor networks in bridge structural monitoring," 2015 IEEE SENSORS, Busan, pp. 1-4, 2015.
- [7] C. Vankecke et al., "Multisource and Battery-Free Energy Harvesting Architecture for Aeronautics Applications," in *IEEE Transactions on Power Electronics*, vol. 30, no. 6, pp. 3215-3227, June 2015.
- [8] Y. K. Tan and S. K. Panda, "Energy Harvesting From Hybrid Indoor Ambient Light and Thermal Energy Sources for Enhanced Performance of Wireless Sensor Nodes," in *IEEE Transactions on Industrial Electronics*, vol. 58, no. 9, pp. 4424-4435, Sept. 2011.
- [9] M. Wahbah, M. Alhawari, B. Mohammad, H. Saleh and M. Ismail, "Characterization of Human Body-Based Thermal and Vibration Energy Harvesting for Wearable Devices," in *IEEE Journal on Emerging and Selected Topics in Circuits and Systems*, vol. 4, no. 3, pp. 354-363, Sept. 2014.
- [10] M. Balato, L. Costanzo and M. Vitelli, "MPPT in Wireless Sensor Nodes Supply Systems Based on Electromagnetic Vibration Harvesters for Freight Wagons Applications," in *IEEE Transactions on Industrial Electronics*, vol. 64, no. 5, pp. 3576-3586, May 2017.
- [11] T. Wu, F. Wu, J. M. Redouté and M. R. Yuce, "An Autonomous Wireless Body Area Network Implementation Towards IoT Connected Healthcare Applications," in *IEEE Access*, vol. 5, pp. 11413-11422, 2017.
- [12] T. Jang et al., "Circuit and System Designs of Ultra-Low Power Sensor Nodes With Illustration in a Miniaturized GNSS Logger for Position Tracking: Part I—Analog Circuit Techniques," in *IEEE Transactions on Circuits and Systems I: Regular Papers*, vol. 64, no. 9, pp. 2237-2249, Sept. 2017.
- [13] K. Aono, N. Lajnef, F. Faridazar and S. Chakrabartty, "Infrastructural health monitoring using self-powered Internet-of-Things," in *IEEE International Symposium on Circuits and Systems (ISCAS)*, Montreal, QC, pp. 2058-2061, 2016.
- [14] Z. Zeng, X. Li, A. Bermak, C. Y. Tsui and W. H. Ki, "A WLAN 2.4-GHz RF energy harvesting system with reconfigurable rectifier for wireless sensor network," in *IEEE International Symposium on Circuits and Systems (ISCAS)*, Montreal, QC, pp. 2362-2365, 2016.
- [15] J. MacDonald, "Electric vehicles to be 35% of global new car sales by 2040," *Bloomberg New Energy Finance*, February 25, 2016. [Online]. Available: https://about.bnef.com. [Accessed November 4, 2017].
- [16] M. R. Yemparala, S. Yerabati and G. I. Mary, "Performance analysis of controller area network based safety system in an electric vehicle," in IEEE International Conference on Recent Trends in Electronics, Information & Communication Technology (RTEICT), Bangalore, pp. 461-465, 2016.
- [17] Q. Zhu, M. Quan, and Y. He, "Vibration energy harvesting in automobiles to power wireless sensors," in *Proceedings of the International Conference on Information and Automation (ICIA 2012)*, Shenyang, Liaoning, China, pp. 349–354, 2012.

- [18] M. Tak and M. Setia, "Converting waste heat from automobiles to electrical energy," in *Proceedings of The 7th International Power Electronics and Motion Control Conference*, Harbin, China, pp. 2095-2098, 2012.
- [19] S. Huang and D. Infield, "The potential of domestic electric vehicles to contribute to Power System Operation through vehicle to grid technology," in 2009 44th International Universities Power Engineering Conference (UPEC), Glasgow, pp. 1-5, 2009.
- [20] L. Wu, X.-D. Do, S.-G. Lee, and D.S. Ha, "A Self-powered and Optimal SSHI Circuit Integrated with an Active Rectifier for Piezoelectric Energy Harvesting," *IEEE Transactions on Circuits and Systems I: Regular Papers*, Vol. 64, No. 3, pp.537 – 548, March 2017.
- [21] D. A. Sanchez, J. Leicht, F. Hagedorn, E. Jodka, E. Fazel and Y. Manoli, "A Parallel-SSHI Rectifier for Piezoelectric Energy Harvesting of Periodic and Shock Excitations," in *IEEE Journal of Solid-State Circuits*, vol. 51, no. 12, pp. 2867-2879, Dec. 2016.
- [22] S. Du, Y. Jia, C. D. Do and A. A. Seshia, "An Efficient SSHI Interface With Increased Input Range for Piezoelectric Energy Harvesting Under Variable Conditions," in *IEEE Journal of Solid-State Circuits*, vol. 51, no. 11, pp. 2729-2742, Nov. 2016.
- [23] N. Kong, D. S. Ha, A. Erturk, and D. J. Inman, "Resistive impedance matching circuit for piezoelectric energy harvesting," *Journal of Intelligent Material Systems and Structures*, vol. 21, no. 13, pp. 1293–1302, September 2010.
- [24] N. Kong and D. S. Ha, "Low-Power Design of a Self-powered Piezoelectric Energy Harvesting System With Maximum Power Point Tracking," in *IEEE Transactions on Power Electronics*, vol. 27, no. 5, pp. 2298-2308, May 2012.
- [25] J. H. Hyun, D. S. Ha, D. Daeick Han and C. M. Kyung, "A solar energy harvesting system for a portable compact LED lamp," *IECON 2015 - 41st Annual Conference of the IEEE Industrial Electronics Society*, Yokohama, pp. 001616-001621, 2015.
- [26] M. Alhawari, T. Tekeste, B. Mohammad, H. Saleh and M. Ismail, "Power management unit for multi-source energy harvesting in wearable electronics," 2016 IEEE 59th International Midwest Symposium on Circuits and Systems (MWSCAS), Abu Dhabi, pp. 1-4, 2016.
- [27] S. Bandyopadhyay and A. P. Chandrakasan, "Platform Architecture for Solar, Thermal, and Vibration Energy Combining With MPPT and Single Inductor," in *IEEE Journal of Solid-State Circuits*, vol. 47, no. 9, pp. 2199-2215, Sept. 2012.
- [28] C. Ding, S. Heidari, Y. Wang, Y. Liu and J. Hu, "Multi-source in-door energy harvesting for non-volatile processors," 2016 IEEE International Symposium on Circuits and Systems (ISCAS), Montreal, QC, pp. 173-176, 2016
- [29] I. M. Darmayuda et al., "A Self-Powered Power Conditioning IC for Piezoelectric Energy Harvesting From Short-Duration Vibrations," in *IEEE Transactions on Circuits and Systems II: Express Briefs*, vol. 59, no. 9, pp. 578-582, Sept. 2012.
- [30] Y. Gao, D. I. Made, S. J. Cheng, M. Je and C. H. Heng, "An energy-autonomous piezoelectric energy harvester interface circuit with 0.3V startup voltage," 2013 IEEE Asian Solid-State Circuits Conference (A-SSCC), Singapore, pp. 445-448, 2013.
- [31] D. Niu, Z. Huang, M. Jiang and Y. Inoue, "A sub-0.3V CMOS rectifier for energy harvesting applications," 2011 IEEE 54th International Midwest Symposium on Circuits and Systems (MWSCAS), Seoul, pp. 1-4, 2011.
- [32] E. Belal, H. Mostafa and M. S. Said, "Comparison between active AC-DC converters for low power energy harvesting systems," 2015 27th International Conference on Microelectronics (ICM), Casablanca, pp. 253-256, 2015.
- [33] A. S. Herbawi, O. Paul and T. Galchev, "An ultra-low-power active AC-DC CMOS converter for sub-1V integrated energy harvesting applications," 2013 IEEE SENSORS, Baltimore, MD, pp. 1-4, 2013.
- [34] T. O'Connor, J. H. Hyun and D. S. Ha, "Power management circuit for kinetic energy harvesting from freight railcars," 2017 IEEE 60th International Midwest Symposium on Circuits and Systems (MWSCAS), Boston, MA, pp. 1426-1429, 2017.